

## Effect of micro-patterning on bacterial adhesion on PET (polyethylene terephthalate) surface

Liyun Wang<sup>1,2</sup>, Wei Chen<sup>1,\*</sup>, Eugene Terentjev<sup>2,\*</sup>

<sup>1</sup> School of Food Science and Technology, Jiangnan University, Wuxi 214122, China

<sup>2</sup> Cavendish Laboratory, University of Cambridge, J. J. Thomson Avenue, Cambridge CB3 0HE, UK

\* Corresponding author: Wei Chen, Tel.: +86 0510 85912155; E-mail: [weichen@jiangnan.edu.cn](mailto:weichen@jiangnan.edu.cn)

Eugene Terentjev, Tel.: +44 (0)1223 37003; E-mail: [emt1000@cam.ac.uk](mailto:emt1000@cam.ac.uk)

### Abstract

Bacterial adhesion on surfaces commonly used in medicine and food industry could lead to infections and illnesses. Topographically patterned surfaces recently have shown to be a promising alternative to chemical antibacterial methods, which might release cytotoxin and promote antibiotic resistance. In this study we fabricated micro-patterned polyethylene terephthalate surfaces, and quantitatively explored the amount and localization of *Escherichia coli* MG1655 cells attached on a series of defined topographies. The adhesion was conducted in static conditions and under a weak flow, in both physiological buffer and nutritious solutions. The results showed that in the presence of weak shear force live bacteria could still maintain sensing ability in nutritious culture, but not in buffer solution. The finely textured surface, which could inhibit bacterial adhesion in the early stage of attachment, reversed its effect to enhance the adhesion after 24 h incubation, indicating that microbial cells seemed to be able to sense the disadvantageous condition and eventually overcome it. In terms of adhesion localization, bacteria exhibited preferential adhesion onto the edges of topographic features. The patterned substrates that have the most even (homogeneous) bacterial localization on topographic features retained the least attachment after 24 h exposure.

**Keywords:** Micro-patterning; Polyethylene terephthalate; Bacterial adhesion; Topographic sensing

## 1. Introduction

Bacterial adhesion onto abiotic surfaces is the first step to form biofilms (adherent bacteria colonize and then synthesize polymeric biofilm matrix on the solid surfaces).<sup>1, 2</sup> Most medical devices and food processing facilities are prone to infections caused by the attached microbes, and eventually - biofilms, leading to a direct threat to health and food contamination.<sup>3-6</sup> Hence, a host of biological and chemical strategies have been employed to study bacterial adhesion and develop abiotic surfaces in order to reduce initial surface contamination. These approaches generally involve a chemical surface modification with antibiotics, enzymes or other antimicrobial agents, for instance, covalently bonding the active agents.<sup>4, 5, 7-9</sup> However, the issues of antibiotic resistance in bacterial strains and cytotoxicity of the active agents limit the application of these strategies in medicine and food industry.<sup>1, 10-12</sup> Thus the physical approach, i.e. designing and utilizing special surface topographies as an alternative to traditional chemical strategies, has been increasingly attempted in the last decade.

Surface topographies with regularly shaped surface patterns significantly influence mammalian cell behaviors, which has been well elaborated in literature.<sup>13</sup> In contrast, the mechanism regulating the effect of defined surface features with controlled dimensions and shape on bacterial adhesion has not yet been addressed, since only few studies have focused on bacterial attachment on patterned surfaces. Friedlander et al.<sup>1</sup> and Xu et al.<sup>5</sup> both hypothesized that surface patterns with dimensions smaller than bacterial cell diameter would reduce the surface area accessible to attachment, thus decreasing the bacterial colonization. Xu et al. found a significant decrease in the adhesion of staphylococcal stains on the surfaces with submicron pillars (0.4 and 0.5  $\mu\text{m}$  diameter),<sup>5</sup> while Friedlander et al. reported an initially reduced attachment of *Escherichia coli* (*E.coli*) on the substrates with sub-micrometer crevices (0.4  $\mu\text{m}$  width), reversing to an increased attachment at longer exposure.<sup>1</sup> Whitehead et al. studied the retention of *Staphylococcus aureus* and *Pseudomonas aeruginosa* on pitted surfaces (respectively 0.2, 0.5, 1 and 2  $\mu\text{m}$  pit diameter), and demonstrated that the cells were retained more within larger surface features,<sup>14</sup> but they did not quantitatively characterize the differences of the pits among surfaces. Regarding the distribution of adherent microorganisms on the patterned surfaces, Hsu et al.<sup>3</sup> showed that bacterial cells preferentially localized onto the areas between the pits, rather than inside them. However, the cell lengths of the tested stains in their study were no less than the dimensions of the wells, rendering it a bit difficult to confirm such a conclusion. Hou et al.<sup>15</sup> investigated the topographic patterns which were larger than bacterial cells in every dimension, and found that the valleys (5-20  $\mu\text{m}$  width) between square pillars were more favorable for *E.coli* adhesion even when the dimension of pillars (e.g. 100  $\mu\text{m}$  by 100  $\mu\text{m}$ ) was much larger than valleys. Nevertheless,

1 the high depth of the patterns (10  $\mu\text{m}$ ) led to much space volume available to bacteria, thus contributing to the  
2 clustered cells seen in the valleys. It seems to be not so impartial to compare bacterial adhesion within spaces and  
3 that on plane surfaces, given such length scales. Therefore, the bacterial response to surface topography with  
4 ordered arrays has yet to be carefully studied, and the quantity and location of the adherent cells need to be  
5 analyzed quantitatively.

6 In the earlier literature, the substrates conducted for bacterial attachment were mostly polydimethylsiloxane  
7 (PDMS) and silicon wafers,<sup>1, 3, 15</sup> which could be patterned easily using the well-known and widely applied  
8 techniques in microfluidics, such as photolithography.<sup>13, 16</sup> However, the much more important substrate materials  
9 in medical devices and food industry that are susceptible to microorganisms are stainless steel, ceramic, and  
10 polymers such as polyethylene terephthalate (PET). In this study, PET films were used to investigate the effect of  
11 micro-patterning on the bacterial adhesion, since PET is ubiquitous in food packaging and medical technology, for  
12 instance soft drink bottles, vascular grafts, artificial heart valve closure, implantable sutures and surgical mesh<sup>17, 18</sup>  
13 and it has also been recently applied to fabricate scaffolds in tissue engineering.<sup>19, 20</sup>

14 Considering the applications of PET films in medical technology, topographically engineered PET substrates  
15 should maintain the original (favorable) physicochemical characteristics of PET films, thus rendering them also  
16 applicable in other bioengineered processes.<sup>19</sup> As PET reacts with many chemical developers and absorbs UV  
17 radiation, the standard photolithography would not be applicable for its patterning. Hence, researchers focused on  
18 other methods, such as hot embossing lithography, where a mold is pressed into a PET film at an elevated  
19 temperature.<sup>21, 22</sup> However, the most interesting and relevant length scales (a few micrometers, comparable with  
20 the length scale of bacteria themselves) have never been achieved on PET surfaces. We design topographic  
21 features on the surface such that their characteristic height is comparable with *E.coli* diameter (~0.5 $\mu\text{m}$ ). Our PET  
22 embossing procedure is carried out at a low temperature to avoid chemical and mechanical degradation of PET  
23 (which would occur at high temperatures, leading to a loss of transparency and flexibility<sup>21</sup>) and so require a high  
24 force applied to the polymer melt. This requires a mechanically robust mold for embossing. In our work, we have  
25 developed a technologically robust method of patterning PET films at these length scales using a three-step  
26 procedure to produce a durable epoxy-based mold for hot embossing.

27 We find that at short time of exposure to a substrate, the actively moving cells can still find their preferential  
28 location, even in highly-viscous nutritious medium, and so we found the most and the least preferred patterns for  
29 attachment. However, we also found that the topography that could initially reduce bacterial adhesion, produced  
30 the increased the adhesion after longer (24 h) exposure, an effect we attribute to an active compensation by the

1 bacteria. Regarding the fine detail of topographic features affecting the adhesion, *E.coli* MG1655 was found to  
2 preferentially attach on the edges, especially those with less curvature. The results in this work would be helpful  
3 not only in understanding the microbial response to textured surfaces but also in designing effectively  
4 anti-adhesive PET films.

## 6 **2. Materials and Methods**

### 8 2.1 Materials

9 PET films with a thickness of 0.35 mm were purchased from Goodfellow Cambridge Ltd. (Huntingdon, UK).  
10 The films were cut into small pieces (2.1 cm × 0.8 cm) for experiments and cleaned ultrasonically in 100% ethanol  
11 for 15 min and then in deionized purified water for 15 min. They were then dried under nitrogen. The clean flat  
12 PET surface had been characterized for roughness:  $R_a=5.04\pm0.16$  nm according to wide-area AFM scans, and for  
13 contact angle:  $\theta =69.6\pm0.2^\circ$  with pure deionized water at 20 °C using a contact angle goniometer (KSV CAM 200,  
14 KSV Instruments Ltd., Helsinki, Finland).

### 16 2.2 Fabrication of surface topography

17 We designed and printed micro-patterns with six different dimensions on a quartz photomask (Micro  
18 Lithography Services Ltd, UK). Table 1 shows the shape and dimensions of the patterns. The standard procedure  
19 of UV photolithography<sup>23, 24</sup> was followed to transfer these features onto a silicon wafer spin-coated with a thin  
20 layer of photoresist (SU-8 2000.5 or 3005, MicroChem Corp., MA, USA). Briefly, the spin-coating speed was  
21 3000 or 4000 rpm, respectively, and other photolithographic parameters, such as exposure time of UV light  
22 through the photomask, all followed the instructions of SU-8 datasheet (www. microchem.com). Owing to the  
23 diffraction of UV light, a gradient of height at the fabricated pattern sidewall (edge slope) is inevitable on the layer  
24 of photoresist.<sup>25</sup> In order to reduce the effect of this phenomenon on the microscopic structural features, the  
25 thickness of the photoresist layer should be low, as the dimension of the patterns here was just a few micrometers.  
26 Hence, SU-8 3005 and 2000.5 were applied, whose thicknesses on the wafer could be both down to below 5  $\mu\text{m}$ ,  
27 especially SU-8 2000.5 system could allow the feature depth down to around 0.5  $\mu\text{m}$ . The silicon wafer with the  
28 cured SU-8 pattern would act as the master mold for micro-patterning PET surfaces, as shown in Figure 1a. Then  
29 PDMS (SYLGARD 184 Silicone Elastomer Kit, Dow Corning, Midland, MI, USA) was cast onto the wafer, so  
30 negative patterns could be replicated on the PDMS elastic stamp. This is now a well-known and widely used

1 procedure in microfluidics.<sup>26</sup> The epoxy resin and hardener (Easy Composites Ltd., Staffordshire, UK) were  
2 mixed thoroughly (the mixing ratio 20:7 by weight) and the mixture was cast on the inverted PDMS stamp, Figure  
3 1b, followed by degassing and curing for 24h at room temperature. In order to achieve the required high  
4 temperature characteristics and stability, the epoxy resin mold was subjected to a post cure process (baking at 40,  
5 80, 120 and 160 °C, sequentially, for 1h each). After removal of elastic PDMS stamp, the epoxy mold was ready  
6 for the hot embossing of PET. Specifically, one PET piece was placed on the top of the resin mold, and softened  
7 gently by increasing the temperature at a rate of 0.1 °C/s to 78 °C (just above its  $T_g$ ), before a pressure of 0.5 MPa  
8 was applied for 10 min. After cooling down to below 50 °C, the pressure was released, and the patterned PET film  
9 would de-bond from the epoxy mold automatically. The textured PET samples were then cleaned ultrasonically in  
10 100% ethanol for 15 min and then in deionized purified water for 15 min and dried with nitrogen.

11 The surface topography of micro-patterned PET was characterized using scanning electron microscope (SEM)  
12 (FEI Philips XL30 sFEG, FEI, Hillsboro, USA). The height of features on epoxy molds and patterned PET surfaces  
13 were measured by atomic force microscopy (AFM) (Veeco Dimension 3100) in tapping mode, and AFM images  
14 were analyzed using the open-source software Gwyddion (<http://gwyddion.net/>). The infrared spectra (IR) of PET  
15 (3 μm thick film) before and after hot embossing by a flat mold were recorded using a Fourier transform infrared  
16 spectrometer (Nicolet iS10, Thermo Scientific, USA). Sixty-four scans were performed for data acquisition in the  
17 spectral region 400 cm<sup>-1</sup> to 4000 cm<sup>-1</sup>.

18

### 19 2.3 Bacterial stain and culture

20 A loop of *E.coli* MG1655 stock was streaked onto a Luria broth (LB) agar plate and incubated at 37 °C  
21 overnight. A single colony was then inoculated into a test tube containing 5 mL LB culture media and grown  
22 overnight at 37 °C, with shaking at 200 rpm. A 100 μL of culture was transferred into a fresh tube of 5 mL LB and  
23 incubated with shaking until stationary phase was reached (12-14 h) to obtain the microbial suspension. The  
24 stationary phase culture contained  $\sim 3 \times 10^9$  colony forming units per mL (CFU/mL). To prepare bacterial  
25 suspension in phosphate buffered saline (PBS) buffer, the stationary phase culture was used to harvest bacteria by  
26 centrifugation at 1200g for 5 min, and then the bacterial pellet was washed with 0.01 M PBS and resuspended in 5  
27 mL PBS buffer.

28 To estimate whether the exposure of patterned PET surfaces in bacterial suspension leads to noticeable  
29 modifications of the surface, which would then affect further bacterial adhesion, we tested the variation of contact  
30 angle on such an exposure. A fresh bacterial suspension in PBS buffer was kept stationary at 37 °C for 24 h, before

1 successively passed through 0.2- $\mu$ m filters four times. Then clean PET samples were immersed in this filtered  
2 solution for 24 h at 37 °C. ~~The resulting exposed PET surfaces were washed twice with fresh PBS buffer and then~~  
3 ~~dried at room temperature. These exposed and clean patterned PET surfaces were firstly tested for contact angle.~~  
4 ~~At least 3 measurements per patterned region were taken, registering a decrease by about 10° compared to fresh~~  
5 ~~PET surfaces.~~ Secondly, we compared the adhesion on the freshly cleaned and the exposed PET surfaces which  
6 were statically incubated in a fresh PBS-buffered bacterial suspension for 0.5 h to estimate the amount of attached  
7 cells, ~~and confirmed there was no significant difference (less than 4% difference).~~

#### 9 2.4 Bacterial adhesion assays

10 The clean patterned PET surfaces were sterilized with 70% ethanol for 15 min and rinsed thrice with sterile  
11 water and LB media/PBS buffer. Each sample surface was then vertically placed into a test tube (diameter 2.2 cm)  
12 containing the stationary-phase synchronized bacterial cells suspended in LB culture or PBS solution.

13 Following incubation at 37 °C statically or with shaking at 200 rpm, the surfaces were washed with tris buffered  
14 saline (TBS) buffer thrice, and then incubated for 15 min in the dark with the BacLight Live/Dead viability kit  
15 (Invitrogen, kit no. L7007). The kit was dissolved in TBS buffer at the concentration recommended by the  
16 manufacturer. Samples were then rinsed twice with TBS and immersed into a 50% glycerol solution in TBS before  
17 imaging. Bacteria attached to the surface were then visualized in situ using Confocal Laser Scanning Microscopy  
18 (CLSM) microscope (LEICA TCS SP5) with an oil immersion objective lens at 40 $\times$  magnification, zoom 1:4.9. At  
19 least six fields of view were randomly chosen for analysis. To quantitatively determine the attached cells count  
20 (cells/mm<sup>2</sup>) on varied micro-patterns, the images were analyzed using Image J (NIH, Bethesda, Maryland,  
21 <http://rsbweb.nih.gov/ij/>).

22 In order to investigate the distribution of adherent microorganisms, SEM was also conducted to visualize the  
23 patterned PET surfaces that were statically incubated with bacterial suspension in PBS buffer for 24 h. Specifically,  
24 the attached bacteria were fixed overnight in 2.5% glutaraldehyde in 0.1 M phosphate buffer (pH 7.4) at 4 °C, and  
25 then rinsed three times in 0.1 M PBS solution. Sequentially, specimens were dehydrated in an ethanol series of  
26 25%, 50%, 75%, 95%, 100%, 100%, 100% (vol/vol) ethanol for 10 min each, dried in room temperature, sputter  
27 coated with gold and analyzed with SEM.

28 All statistical analysis was performed using Microsoft Excel (Microsoft Corp., Redmond, WA). Values were  
29 reported in the text as mean value  $\pm$  standard deviation.

### 30 **3. Results**

### 3.1 Embossing micro-patterns on PET at moderate temperature

Generally, the effect of surface topography on bacterial adhesion is quantitatively characterized in terms of total adherent cells. The locational response of attached bacteria to surface configuration has yet to be investigated, however, it is of vital importance to design anti-adhesive patterns on surfaces. Firstly, surface topography with defined configurations is supposed to be well fabricated. We designed and printed micro-patterns with six different dimensions on the photomask. Table 1 shows the shape and dimensions of the patterns. UV lithography was applied to transfer these features from the photomask to the layer of photoresist spin-coated on silicon wafers. Owing to the diffraction of UV light, a gradient of height at the fabricated pattern sidewall (edge slope) is inevitable on the layer of photoresist. In order to reduce the effect of this phenomenon on the microscopic structural features, the thickness of the photoresist layer should be low, as the dimension of the patterns here was just a few micrometers. Hence, SU-8 3005 and 2000.5 were applied, whose thicknesses on the wafer could be both down to below 5  $\mu\text{m}$ . After the replication from the PDMS stamp, micro-scale patterns were transferred on the surface of epoxy resin mold. Surface topography with defined configurations was well fabricated. Figure 2a shows the AFM image of the resulting epoxy mold (the No. 6-pattern, the dimension is shown in Table 1). The depth profiles of the molds produced using photoresists SU-8 3005 and 2000.5 were obtained from the cross-section of AFM image, showing that the depths were 3.29 and 0.65  $\mu\text{m}$ , respectively (Figure 2b). Due to the shape of AFM tip on the cantilever, the image was some combination of the tip shape and the true surface topography, thus the depth profile of SU-8 3005 at the edge slope between the top and bottom surface is a bit different from that of SU-8 2000.5. After hot embossing, the micro-patterns were reliably replicated from both molds onto PET films, as revealed in SEM images (Figure 2c-d). In this study, we chose SU-8 2000.5 to micro-pattern PET films for bacterial adhesion assays. As shown in Figure 3, the morphology of all six patterned areas was verified by SEM. The inserted profile in Figure 3 (No.6) shows the height of the pillars that is approximately 0.65  $\mu\text{m}$ . It could be seen that the topographic features on patterned PET surfaces simultaneously include curved and straight edges, flat plateaus (top of pillars), and flat surfaces between pillars so as to explore the bacterial behavior on surfaces with different topographies.

Infrared spectroscopy (IR) and contact angle measurements of PET films before and after hot embossing were carried out in order to assess the impact of our treatment procedure on PET physicochemical properties, which might affect the behavior of bacteria on the surface. We found that the micro-patterned PET surface did not exhibit any chemical changes (~~IR data not shown~~Figure 4a), due to the low-temperature embossing procedure. Similarly,

1 hot-embossing PET by a flat mold led to a surface with almost unchanged contact angle ( $71.4 \pm 1.0^\circ$ , after hot  
2 embossing). ~~As demonstrated in Figure 4b,~~ the micro-patterned PET areas had a slightly different contact angle,  
3 generally increasing in patterns with smaller size features. We then further tested how the contact angle would  
4 vary on 24 h exposure of PET to a broth of chemicals from a filtered mature bacterial suspension. In all surfaces,  
5 the contact angle was found slightly decreased by about  $10^\circ$ , i.e. surfaces became slightly less hydrophobic  
6 (Figure 4).

7 Notably, the six rod-patterned areas with different features were simultaneously replicated onto the same PET  
8 sample surface, thus rendering all textured regions exposed in an identical bacterial suspension. The bacterial  
9 adhesion results were shown as follows.

### 11 **4.3.2 Bacterial adhesion on micro-patterned PET surfaces**

#### 12 3.2.1 Initial adhesion of *E.coli* on PET surfaces

13 ~~Bacterial adhesion on abiotic surfaces is thought to be dominated by the bacteria-surface interactions that~~  
14 ~~highly depend on the chemical and topographical properties of substrate surfaces. Additionally, owing to the~~  
15 ~~presence of fimbriae or pili appendages in *E.coli* cells, which are susceptible to environmental conditions such as~~  
16 ~~culture media, their aid in the initial attachment to PET surfaces is also supposed to be considered.~~ We examined  
17 bacterial initial adhesion to patterned and flat PET films in nutritious culture (LB medium) and in oligotrophic  
18 solution (PBS buffer), both statically and dynamically (shaking at 200rpm). A comment on the ‘dynamic  
19 conditions’ is due here. Taking the dimensions and the rate of shaking device, we have estimated the magnitude of  
20 the local flow disturbance in the zone of bacterial adhesion. In the case of flat PET surface the shaking induces the  
21 local shear rate of  $\sim 10 \text{ s}^{-1}$ , or the stress  $\sigma \sim 0.01 \text{ Pa}$ . Even though these values would change with the patterned  
22 surface (reduce in the corners of pillars), it is important to note the very low level of shear stress in our ‘dynamic  
23 attachment’ regime (in further work we will specifically report the effect of increasing shear on bacteria  
24 attachment). The patterned PET surfaces were immersed in *E.coli* MG1655 suspensions (i.e. bacterial cells  
25 suspended in LB medium or PBS buffer) for 0.5 h and then imaged using CLSM. The representative fluorescence  
26 images are shown in Figure 5. ~~To quantitatively determine the attached cells count ( $\text{cells}/\text{mm}^2$ ) on varied~~  
27 ~~micro-patterns, these images were analyzed using Image J.~~ Figures 6-7 show the statistical analysis of the  
28 bacterial adhesion on these patterns, respectively illustrating the number of adherent bacteria on textured PET  
29 surfaces in the environment of LB culture medium and PBS buffer, and the relative proportions of live and dead  
30 cells retained on the surfaces are also presented.



1 In the initial stage of microbial adhesion in the nutritious environment, *E.coli* achieved a better adhesion in the  
2 presence of shaking for both live and dead cells, as demonstrated by a higher level of attachment on the surfaces  
3 than that in static condition (Figure 6a). No dead cells but only live cells were observed to attach on PET surfaces  
4 when the sample was cultured in bacterial suspensions statically, while some dead cells could still adhere onto the  
5 surfaces when a weak shear force was applied (i.e. when the PET sample incubated in the bacterial suspension was  
6 kept in a shaker). ~~The bacterial movement in the suspension is necessary in order to come in the initial contact~~  
7 ~~with the surface, thus live cells appeared to behave actively to reach PET surfaces, since live cell movement could~~  
8 ~~be mediated through fimbriae or flagella. In a mild fluid flow, the dead bacteria (like colloid particles) did~~  
9 ~~accidentally touch the surface, so we found some number of them in the images.~~ As seen in Figure 6a, the least  
10 attachment of dead cells was seen on the flat surface, and the maximum difference between the proportion of live  
11 cells and that of dead cells adherent was also observed on the smooth surface (Figure 6b), indicating that the  
12 adherence of dead cells seemed to benefit from PET patterning, where the local turbulence of fluid flow should  
13 form pockets of favored contact.

14 In contrast, when *E.coli* were suspended in PBS buffer, the flow over the patterned surface did decrease the total  
15 numbers of attached cells (Figure 7a), which is consistent with the results by other investigators using similar  
16 conditions.<sup>27</sup> Dead cells could adhere onto PET surface when the adhesion process was performed statically, and  
17 ~~Less~~ difference between the proportion of live cells and that of dead cells adherent were observed in the dynamic  
18 conditions (Figure 7b). ~~We also found more of the live cells accumulated in the dynamic than in static suspensions~~  
19 ~~in each of the patterns.~~ Interestingly, as shown in Figure 6a, the amounts of live cells adhered under both static and  
20 dynamic conditions exhibited almost the same trend with the pattern number ranging from 1 to 6, ~~which might~~  
21 ~~deserve attention since it revealed that in nutritious conditions a weak shear force would not change the~~  
22 ~~preferential attachment of live bacteria.~~ However, this phenomenon was not pronounced when the surfaces were  
23 challenged with *E.coli* suspended in PBS buffer (Figure 7a), ~~suggesting that when bacteria cultured in~~  
24 ~~oligotrophic solution, microbial movement of live cells is likely to be strongly affected by medium flow.~~

25 Compared with control flat surfaces, the most significant reduction in total amount of adherent bacterial cells  
26 was found on No.1-patterned PET surfaces under static/dynamic conditions in both LB medium and PBS buffer.

#### 28 4.23.2.2 Adhesion of *E.coli* on PET surfaces at 24 h

29 In order to identify whether No.1-patterned surface configuration would still inhibit bacterial adhesion after  
30 long-time exposure, we investigated the attachment on the patterned PET surfaces incubated in PBS-buffered

1 bacterial suspension over 24h using CLSM. Here we did not study the 24h-adhesion in LB culture medium, since  
2 the growth curve of *E.coli* in this nutritious environment has reached stationary phase. Therefore, the conditions  
3 for bacterial movement and attachment are no longer comparable with the short-time data. Figure 8 illustrates the  
4 average numbers of total cells attached to each type of patterned substrate after 24 h incubation. Surprisingly, in  
5 the static condition, the No.1-patterned configuration did not prevent bacterial adhesion (as was the case in a  
6 short-time test, after 0.5 h) but instead has shown the highest numbers of attached bacteria. A similar phenomenon,  
7 that some patterned substrate inhibited microbial attachment at early time points but not later, was also reported by  
8 Friedlander et al..<sup>1</sup> They suggested that it was due to a so-called lotus-leaf wetting state,<sup>28</sup> rendering the patterned  
9 surface non-wetting in the initial stage of adhesion. To test this proposal, we observed the No.1-patterned PET  
10 surfaces microscopically during the early adhesion process, and found that the surfaces were immediately wetted  
11 once they got immersed in the bacterial suspensions, therefore, we had to dismiss the idea of temporary  
12 de-wetting.

13 In this study, we saw a change of PET surface properties over the whole adhesion process, as illustrated by a  
14 drift in the contact angle (i.e. surface tension, Figure 4**b**). Therefore, we immersed one clean patterned PET film in  
15 filtered culture medium for 24 h as described in section 2.3. Then the resulting PET sample was incubated in  
16 *E.coli* PBS-buffered suspension for 0.5 h. The amount of total cells attached to the treated No.1-patterned surface  
17 was  $(2.7\pm 0.4) \times 10^3$  cells/mm<sup>2</sup>, which did not have any significant difference from that without the pre-treatment  
18 by 24 h immersion:  $(2.8\pm 0.2) \times 10^3$  cells/mm<sup>2</sup>, shown in Figure 7(a). It means that the change of contact angle (at  
19 least in the range between 85° and 70°) would not strongly influence bacterial adhesion on the No.1-patterned  
20 surfaces. Hence the reason of the phenomenon of delayed adhesion seems to be solely due to the bacteria  
21 themselves, which will be discussed [Section 5 later](#). It could also be seen from [Figures](#): 7 and 8 that the effect of  
22 shaking disruption on bacterial adhesion was continuing.

23 ~~In terms of the location of bacteria to the regular topography. As mentioned before, the localization of bacteria~~  
24 ~~on the surface topography is also of vital importance. In order to determine the bacterial distribution on the surface~~  
25 ~~features, a visualization of the attached cells on the defined topographies was conducted using SEM (Figure 9). It~~  
26 could be seen that many of the adherent bacteria on No.1-patterned surface were in clusters. As shown in Figures.  
27 10-11, the bacterial location within the diverse topographies was quantitatively analyzed from the SEM images.  
28 Figure 10a demonstrates the total amounts of bacteria retained on the patterns. The trend of total cell numbers with  
29 patterns ranging from No.1 to No.6 appears to be consistent with the results obtained from CLSM (Figure 8), even  
30 though the imaged surfaces came from two different tests. These results both tell that the most attachment after a

1 long exposure occurred in the No.1-patterned area, while the least adhesion occurred in the No.5-patterned region.

2 To better understand the bacterial distribution, firstly, we divided the features into edges (i.e. edges of the  
3 semi-circles and line segments) and flat surfaces (flat areas in patterned regions). Generally, as the flat area  
4 occupied most of the whole patterned surface, a larger proportion of adhesive cells was naturally present on the  
5 flat surfaces (Figure 10b). Hence, to make the meaningful comparison of bacterial attachment onto the edges and  
6 flat surfaces, we introduced the ‘edge area’ equaling the total side length of patterns in SEM image multiplied by  
7 the average width of bacteria (0.5  $\mu\text{m}$ , measured the cells in SEM images using Image J), and used this in  
8 normalizing the results. The total flat area was represented by the whole field area of SEM image with the edge  
9 area subtracted. Figure 11a displays the properly normalized density of attached cells on the edge area and flat  
10 area, which demonstrates a significantly higher level of bacterial adhesion on edges than that on smooth areas for  
11 each type of patterned surface. It reveals a preferential adhesion of *E.coli* onto the edges of patterns.

12 In addition, the density of bacteria retained on the edges (DBE) was found to be strongly dominated by the  
13 shape of edge features. As shown in the insets of Figure 11a, when the curvature radius was 1  $\mu\text{m}$ , DBE sharply  
14 increased with the length of the line segment (i.e. side length, L in Table 1) rising from 1 to 4  $\mu\text{m}$ , before it slowly  
15 increased when L was larger than 4  $\mu\text{m}$ , and when the side length was 4  $\mu\text{m}$ , DBE dramatically raised with the  
16 curvature radius increasing from 1 to 4  $\mu\text{m}$ . It indicates that *E.coli* cells were more likely to attach to the edges  
17 with less curvature.

18 In order to explore the reason why the least adhesion was found on No.5-patterned surfaces, we conducted a  
19 more detailed analysis of bacterial distribution on the surface topographies. As seen in Figure 11b, the edges were  
20 divided into the edges of the semi-circles and line segments separately, and the flat surfaces were partitioned into  
21 three flat areas  $S_1$ ,  $S_2$ , and  $S_3$  (shown in the inset of Figure 11b). The most dramatic difference between the  
22 No.5-patterned surfaces and other ones is that the adhesion localization of bacterial cells on these five parts of  
23 features is more even, that is, there appears to be less preferential attachment in No.5-patterned areas.

## 24 25 **5.4. Discussion**

26 ~~Micro-scale patterns with varied dimensions were fabricated onto PET surfaces and the topographic features~~  
27 ~~simultaneously included curved and straight edges, flat plateaus (top of pillars) and flat valleys between pillars.~~  
28 ~~We characterized bacterial adhesive response to these diversely textured PET surfaces in terms of the numbers of~~  
29 ~~attached cells and the location of bacteria to the regular topography, respectively.~~

30 Bacterial adhesion on abiotic surfaces is thought to be dominated by the bacteria-surface interactions that

1 highly depend on the chemical and topographical properties of substrate surfaces.<sup>13</sup> Additionally, owing to the  
2 presence of fimbriae or pili appendages in *E.coli* cells, which are susceptible to environmental conditions such as  
3 culture media,<sup>29</sup> their aid in the initial attachment to PET surfaces is also supposed to be considered.

4 Firstly, we were interested in the effect of environmental conditions on the bacterial adhesion, specifically the  
5 role of culture medium and the weak medium flow. Previous research usually claimed that the flow of medium  
6 over the substrates would reduce the amount of attached cells.<sup>5, 15, 27</sup> However, based on the results of initial  
7 adhesion, it appears that the role of medium flow in bacteria-surface interactions should take into account the type  
8 of culture medium (nutritious or oligotrophic) and, therefore, the specific bacterial activity in it. We were  
9 convinced that the flow was supposed to affect the bacterial adhesion in two ways: on the one hand, it did provide  
10 some shear force to remove bacteria from surfaces; on the other hand, the flow would also enhance the  
11 opportunities of microbial cells to meet the surfaces. Of course, much depends on the magnitude of shear flow, and  
12 we found that the conditions imposed in a standard cell-culture shaker happen to provide a sufficiently weak shear.

13 ~~During the initial adhesion process, *E.coli* achieved a better adhesion in the presence of shaking when cultivated in~~  
14 ~~LB culture medium, as demonstrated by a higher level of attachment on the surfaces for both live and dead cells~~  
15 ~~than that in static condition (Figure 6a). In contrast, when *E.coli* were suspended in PBS buffer, the flow over the~~  
16 ~~patterned surface did decrease the total numbers of attached cells (Figure 7a), which is consistent with the results~~  
17 ~~by other investigators using similar conditions. Hence, it appears that the role of medium flow in bacteria-surface~~  
18 ~~interactions should take into account the type of culture medium (nutritious or oligotrophic) and, therefore, the~~  
19 ~~specific bacterial activity in it.~~

20 The bacterial movement in the suspension is necessary in order to come in the initial contact with the surface,  
21 thus live cells appeared to behave actively to reach PET surfaces, since live cell movement could be mediated  
22 through fimbriae or flagella. Hence only live bacteria were observed on the PET surfaces in static LB culture  
23 medium. In a mild fluid flow, the dead bacteria (like colloid particles) did accidentally touch the surface, so we  
24 found some number of them in the images. Dead cells could adhere onto PET surface when the adhesion process  
25 was performed statically in PBS buffer environment. It might be because the viscosity of PBS solution is less than  
26 that of LB medium containing concentrated amino acids and peptides, and therefore the increased range of  
27 Brownian motion of dead cells allowed them to come in accidental contact with the surfaces.<sup>30</sup>

28 The comparison of culture media and medium flow is also helpful to get a better insight into the bacterial  
29 surface sensing. With pattern number ranging from No.1 to No.6, the same tendency of changes in amount of  
30 settled live microorganisms was found in nutritious environment both dynamically and statically, and also in

1 non-nutritious solution statically, indicating that *E.coli* live cells are not passive tracers.<sup>31</sup> In LB culture medium,  
2 live cells do not trend to behave like colloid particles that are strongly affected by the shear flow in the  
3 environment. It seems that they could still exhibit their own preference for adherence to the micro-topographic  
4 surfaces even when some shear forces exist. However, when the shaking was conducted in solution without  
5 nutrition (PBS buffer in this study), the active preference to the textured surfaces could not be observed. Why live  
6 bacteria could still selectively and preferentially settle on the patterned substrates with the presence of shaking in  
7 nutritious medium, but not in non-nutritious solution? This might be due to fimbriae/pili, the bacterial cell  
8 appendages mediating microbial adhesion onto abiotic surfaces.<sup>30</sup> As has been noted in the literature, the fimbriae  
9 of *E.coli* MG1655 could be regulated by environmental conditions, such as culture media.<sup>29</sup> It appears that in the  
10 nutritious environment the fimbriae are fully developed on the cell surface, while they might be lost from cell  
11 surface, or made temporarily unfunctional, when bacteria are suspended in non-nutritious medium with the  
12 presence of weak flow, thus rendering the live bacterial cells susceptible to the medium flow and easily removed  
13 from the surfaces. The dead cells in nutritious and non-nutritious environments both behave like colloid particles,  
14 undergoing Brownian motion strongly influenced by environmental conditions, such as medium flow and  
15 viscosity.

16 The quantitative results of total adherent cells demonstrated that our patterns do influence *E.coli* attachment  
17 behavior. The No.1-textured surface, which could be the most potential to inhibit bacterial adhesion, ~~since it was~~  
18 ~~found difficult to accommodate the cells, based on the initial settlement of microorganisms on PET surfaces~~  
19 ~~(Figures. 6-7). Nevertheless, , the No.1 patterned area~~ has instead retained the highest number of cells after being  
20 challenged by bacterial suspension for 24 h, ~~as demonstrated independently by both CLSM and SEM results.~~ The  
21 wetting state of surfaces and changes of contact angle could not explain this phenomenon as Friedlander et al.  
22 attempted,<sup>1</sup> however, the cell clusters ~~(Figure 9, No.1)observed in No.1-patterned surface~~ suggest that this pattern  
23 was likely to form topographic stimuli to bacteria. In the early stage, the cells were hard to get in, but once some  
24 cells anchored, these settled cells might make an effort to mask this disadvantageous surface topography,  
25 meanwhile fimbriae could also be produced more in response to this environmental stimulus,<sup>32</sup> thus facilitating  
26 further microbial attachment.

27 ~~The comparison of the density of bacterial cells occurring at ‘edge area’ and flat area shows preferential~~  
28 ~~adhesion of *E.coli* onto the edges of patterns the locational response of *E.coli* to surface defined configurations~~  
29 ~~(Figure 11a). reveals that Bbacteria seem to be able to sense the topography and preferred to attach the edges of~~  
30 ~~patterns, suggesting that they tended to align in the way that would enhance the cell-surface contact area to anchor~~

1 themselves better, which was also suggested in previous research.<sup>3,33</sup> Another evidence of bacterial active sensing  
2 ability towards the surface configuration could be seen in Figure 9 (No. 5-6), visually showing the microbial  
3 adhesion at the surrounding regions near the boundary between the control and patterned area. In static conditions,  
4 it appears that the microorganisms could distinguish where the patterns were and attempted to preferentially  
5 adhere onto edges, as often claimed in the literature.<sup>15</sup> Such selective adhesion could lead to an uneven distribution  
6 of adherent cells, which might contribute to a higher level of bacterial contamination on patterned surfaces than  
7 that on control surfaces. The dimensions of the No. 5 pattern in our study seem to be a threshold for relatively even  
8 localization of microorganisms, thus less preferential attachment would suppress the total amount of adherent  
9 cells. In terms of the bacterial distribution along the curved and straight edges, owing to the rigid cell shape, they  
10 are much less deformable than eukaryotic cells,<sup>13</sup> therefore, the rod shaped *E.coli* cells were more likely to attach  
11 the less curved edges to avoid deformation of cells.

## 13 **6.5. Conclusion**

14  
15 We have developed a versatile method useful for reproducible fabrication of patterned PET surfaces.  
16 Micro-patterning on a length scale comparable with the bacterial dimensions does have a significant effect on  
17 *E.coli* adhesive behavior on PET surfaces. Bacterial cells preferred to attach to the straight edges of topographic  
18 features, inspiring us to apply more curvature in the designing anti-adhesive bacterial surfaces and coatings  
19 configurations. On the other hand, we found that the effect of changing contact angle (and thus, the wetting on the  
20 surface) has less effect on cell adhesion, compared to topography. Rich culture medium had a strong effect of  
21 bacterial fimbriae mediating the surface activity of live bacteria, while in oligotrophic environment the fimbriae  
22 functionality did not have an effect on *E.coli* adhesion. Our study might also be helpful if the antibiotics and other  
23 antimicrobial agents have to be combined with substrate surfaces: implanting these ~~chemicals~~ mainly on the edges  
24 of topographies would simultaneously reduce the dosages and increase effectiveness of these agents.

## 26 **Acknowledgements**

27 The authors are grateful to Dr. Thomas Müller and Dr. Eileen Nugent for the help with the UV lithography and  
28 bacterial culture, and many valuable discussions. Financial support from China Scholarship Council and Unilever  
29 Corporate Research is acknowledged.

1   **References**

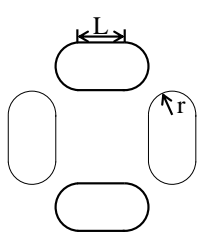
- 2   1. Friedlander RS, Vlamakis H, Kim P, et al. Bacterial flagella explore microscale hummocks and hollows to  
3   increase adhesion. P Natl Acad Sci USA 2013;110:5624-9.
- 4   2. Rizzello L, Sorce B, Sabella S, et al. Impact of nanoscale topography on genomics and proteomics of adherent  
5   bacteria. ACS Nano 2011;5:1865-76.
- 6   3. Hsu LC, Fang J, Borca-Tasciuc DA, et al. Effect of micro-and nanoscale topography on the adhesion of  
7   bacterial cells to solid surfaces. Appl Environ Microb 2013;79:2703-12.
- 8   4. Antoci Jr V, Adams CS, Parvizi J, et al. The inhibition of *Staphylococcus epidermidis* biofilm formation by  
9   vancomycin-modified titanium alloy and implications for the treatment of periprosthetic infection. Biomaterials  
10   2008;29:4684-90.
- 11   5. Xu L-C, Siedlecki CA. Submicron-textured biomaterial surface reduces staphylococcal bacterial adhesion and  
12   biofilm formation. Acta Biomater 2012;8:72-81.
- 13   6. Eichler M, Katzur V, Scheideler L, et al. The impact of dendrimer-grafted modifications to model silicon  
14   surfaces on protein adsorption and bacterial adhesion. Biomaterials 2011;32:9168-79.
- 15   7. Antoci V, King SB, Jose B, et al. Vancomycin covalently bonded to titanium alloy prevents bacterial  
16   colonization. J Orthopaed Res 2007;25:858-66.
- 17   8. Yuan S, Wan D, Liang B, et al. Lysozyme-coupled poly (poly (ethylene glycol) methacrylate)– stainless steel  
18   hybrids and their antifouling and antibacterial surfaces. Langmuir 2011;27:2761-74.
- 19   9. Shi Z, Neoh K, Kang E. Antibacterial activity of polymeric substrate with surface grafted viologen moieties.  
20   Biomaterials 2005;26:501-8.
- 21   10. Campoccia D, Montanaro L, Arciola CR. The significance of infection related to orthopedic devices and  
22   issues of antibiotic resistance. Biomaterials 2006;27:2331-9.
- 23   11. Stewart PS, William Costerton J. Antibiotic resistance of bacteria in biofilms. Lancet 2001;358:135-8.
- 24   12. Threlfall EJ, Ward LR, Frost JA, et al. The emergence and spread of antibiotic resistance in food-borne  
25   bacteria. Int J Food Microbiol 2000;62:1-5.
- 26   13. Anselme K, Davidson P, Popa A, et al. The interaction of cells and bacteria with surfaces structured at the  
27   nanometre scale. Acta Biomater 2010;6:3824-46.
- 28   14. Whitehead KA, Colligon J, Verran J. Retention of microbial cells in substratum surface features of micrometer  
29   and sub-micrometer dimensions. Colloid Surface B 2005;41:129-38.
- 30   15. Hou S, Gu H, Smith C, et al. Microtopographic patterns affect Escherichia coli biofilm formation on poly

- 1 (dimethylsiloxane) surfaces. *Langmuir* 2011;27:2686-91.
- 2 16. Anderson JR, Chiu DT, Wu H, et al. Fabrication of microfluidic systems in poly (dimethylsiloxane).  
3 *Electrophoresis* 2000;21:27-40.
- 4 17. Shirakura A, Nakaya M, Koga Y, et al. Diamond-like carbon films for PET bottles and medical applications.  
5 *Thin Solid Films* 2006;494:84-91.
- 6 18. Li P, Cai X, Wang D, et al. Hemocompatibility and anti-biofouling property improvement of poly (ethylene  
7 terephthalate) via self-polymerization of dopamine and covalent graft of zwitterionic cysteine. *Colloid Surface B*  
8 2013;110:327-32.
- 9 19. Ajallouieian F, Lim ML, Lemon G, et al. Biomechanical and biocompatibility characteristics of electrospun  
10 polymeric tracheal scaffolds. *Biomaterials* 2014;35:5307-15.
- 11 20. Bisson I, Kosinski M, Ruault S, et al. Acrylic acid grafting and collagen immobilization on poly (ethylene  
12 terephthalate) surfaces for adherence and growth of human bladder smooth muscle cells. *Biomaterials*  
13 2002;23:3149-58.
- 14 21. Cecchini M, Signori F, Pingue P, et al. High-resolution poly (ethylene terephthalate)(PET) hot embossing at  
15 low temperature: thermal, mechanical, and optical analysis of nanopatterned films. *Langmuir* 2008;24:12581-6.
- 16 22. Ishizawa N, Idei K, Kimura T, et al. Resin micromachining by roller hot embossing. *Microsyst Technol*  
17 2008;14:1381-8.
- 18 23. Jo B-H, Beebe DJ. Fabrication of three-dimensional microfluidic systems by stacking molded  
19 polydimethylsiloxane (PDMS) layers. *Symposium on Micromachining and Microfabrication: International*  
20 *Society for Optics and Photonics*; 1999. p. 222-9.
- 21 24. Gates BD, Xu Q, Love JC, et al. Unconventional nanofabrication. *Annu Rev Mater Res* 2004;34:339-72.
- 22 25. Levinson HJ. *Principles of lithography*. 2nd ed: SPIE press; 2005. p. 7-9.
- 23 26. Jo B-H, Van Lerberghe LM, Motsegood KM, et al. Three-dimensional micro-channel fabrication in  
24 polydimethylsiloxane (PDMS) elastomer. *J Microelectromech Syst* 2000;9:76-81.
- 25 27. Shive MS, Hasan SM, Anderson JM. Shear stress effects on bacterial adhesion, leukocyte adhesion, and  
26 leukocyte oxidative capacity on a polyetherurethane. *J Biomed Mater Res* 1999;46:511-9.
- 27 28. Barthlott W, Neinhuis C. Purity of the sacred lotus, or escape from contamination in biological surfaces. *Planta*  
28 1997;202:1-8.
- 29 29. Gally D, Bogan J, Eisenstein B, et al. Environmental regulation of the fim switch controlling type 1 fimbrial  
30 phase variation in *Escherichia coli* K-12: effects of temperature and media. *J Bacteriol* 1993;175:6186-93.



1 30. Hori K, Matsumoto S. Bacterial adhesion: from mechanism to control. *Biochem Eng J* 2010;48:424-34.  
 2 31. Hernandez-Ortiz JP, Stoltz CG, Graham MD. Transport and collective dynamics in suspensions of confined  
 3 swimming particles. *Phys Rev Lett* 2005;95:204501.  
 4 32. Kirkpatrick CL, Viollier PH. Reflections on a sticky situation: how surface contact pulls the trigger for  
 5 bacterial adhesion. *Mol Microbiol* 2012;83:7-9.  
 6 33. Whitehead KA, Verran J. The effect of surface topography on the retention of microorganisms. *Food Bioprod*  
 7 *Process* 2006;84:253-9.

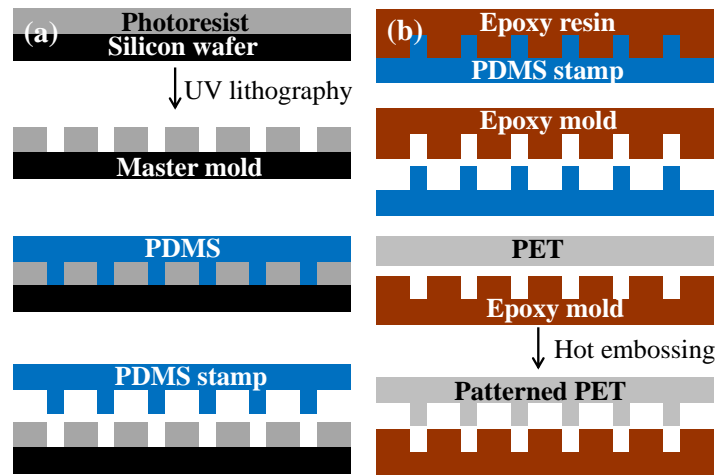
8  
9  
10  
11  
12  
13  
14  
15 Table 1. Geometric characteristics of patterns on PET surfaces

	Pattern	r (radius, $\mu\text{m}$ )	L (side length, $\mu\text{m}$ )	Curvature <sup>a</sup>	Average edge <sup>b</sup> ( $\text{mm}/\text{mm}^2$ )
	No.1	1	1	0.76	335.1 $\pm$ 2.8
	No.2	1	2	0.61	319.6 $\pm$ 1.2
	No.3	1	4	0.44	279.2 $\pm$ 5.0
	No.4	1	8	0.28	238.7 $\pm$ 8.8
	No.5	2	4	0.61	246.9 $\pm$ 6.1
	No.6	4	4	0.76	185.9 $\pm$ 7.4

16 <sup>a</sup> defined as the proportion of semi-circle length in one pattern feature length, i.e.  $2\pi r/(2\pi r+2L)$

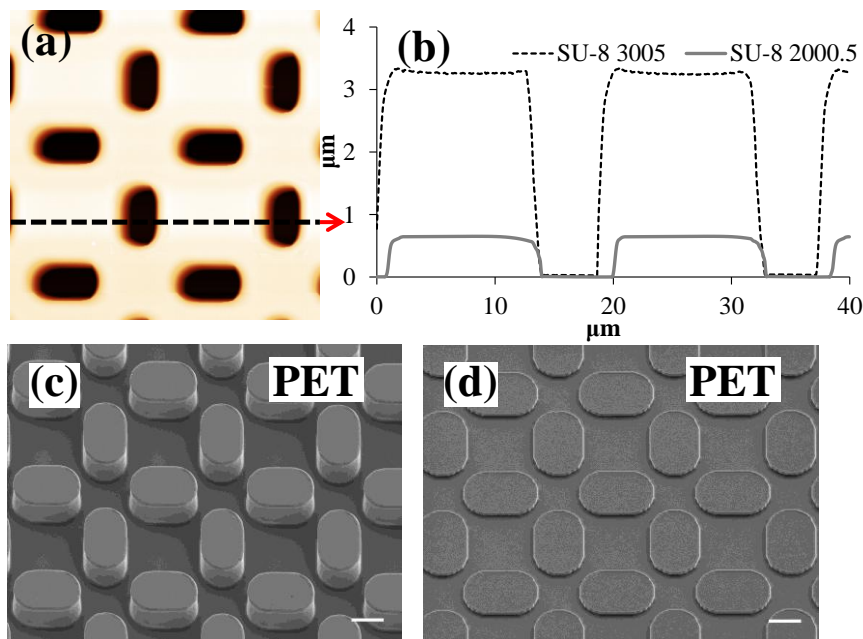
17 <sup>b</sup> total edge length divided by total area in each SEM image (e.g. Figures 3 and 9) of patterned PET surfaces. The total area is  
 18  $3.01 \times 10^{-3} \text{ mm}^2$  measured by Image J. The standard deviation can be obtained since at least five images were randomly taken  
 19 for each pattern.

1



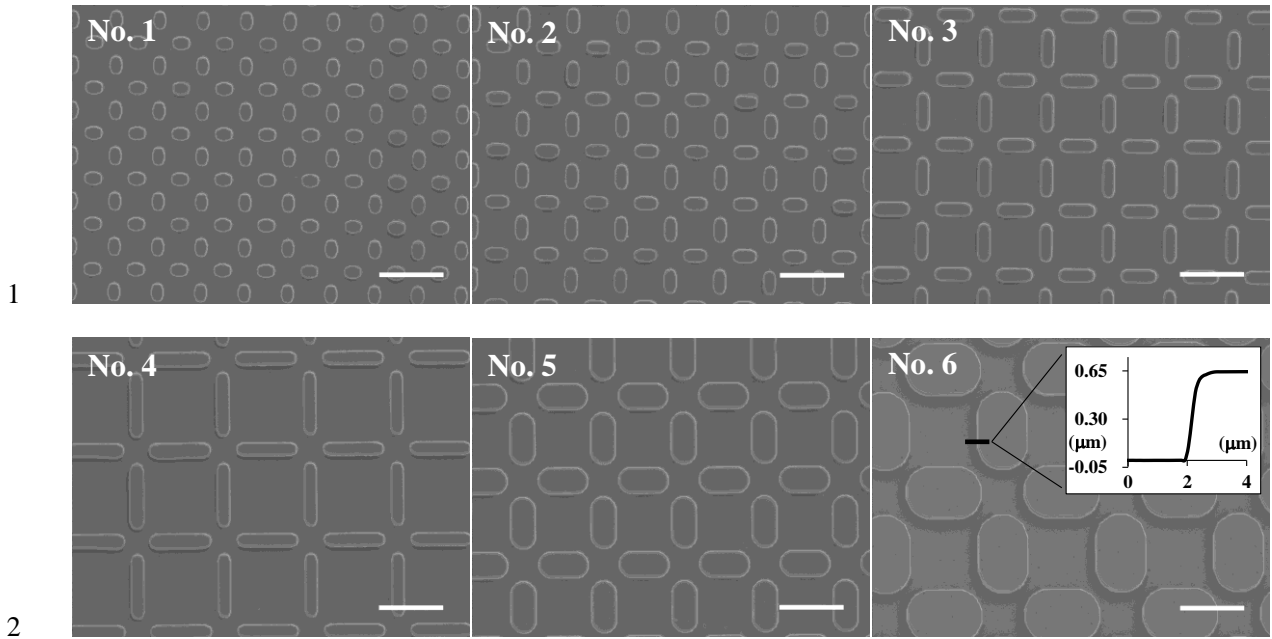
2  
3  
4  
5  
6  
7  
8  
9

**Figure 1.** Schematic diagram illustrating the methodology for surface texturing PET. (a) The UV-lithographic production of a soft PDMS stamp. (b) The fabrication of the durable epoxy mold and the patterning of PET.



10  
11  
12  
13  
14  
15  
16  
17

**Figure 2.** (a) AFM image of the epoxy mold surface prepared using the No.6-pattern in Table 1. (b) The cross section of the profiles in (a) i.e., the height profile along the dotted line. (c-d) SEM images of PET surfaces after hot embossing. Patterns were exactly the same, No.6, but (d) was produced from the master template with SU-8 2000.5, leading to a smaller height (0.65 μm) compared to (c) made with SU-8 3005 (3.29 μm); scale bar: 5 μm.



7

8

**Figure 3.** SEM images of micro-patterned PET surfaces with six different dimensions as shown in Table 1. Scale bar, 10  $\mu\text{m}$ . The inset in No.6 image is the height profile of pillars measured by AFM, confirming the reproducible depth of features.

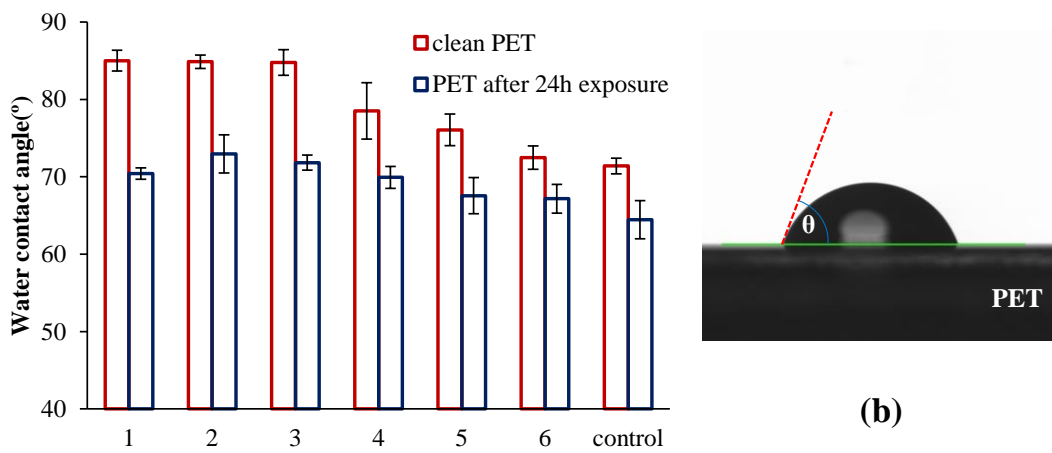
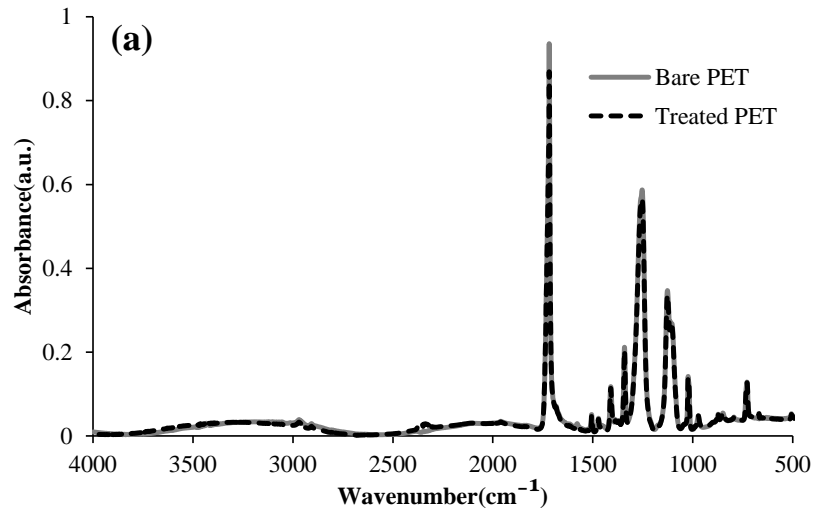
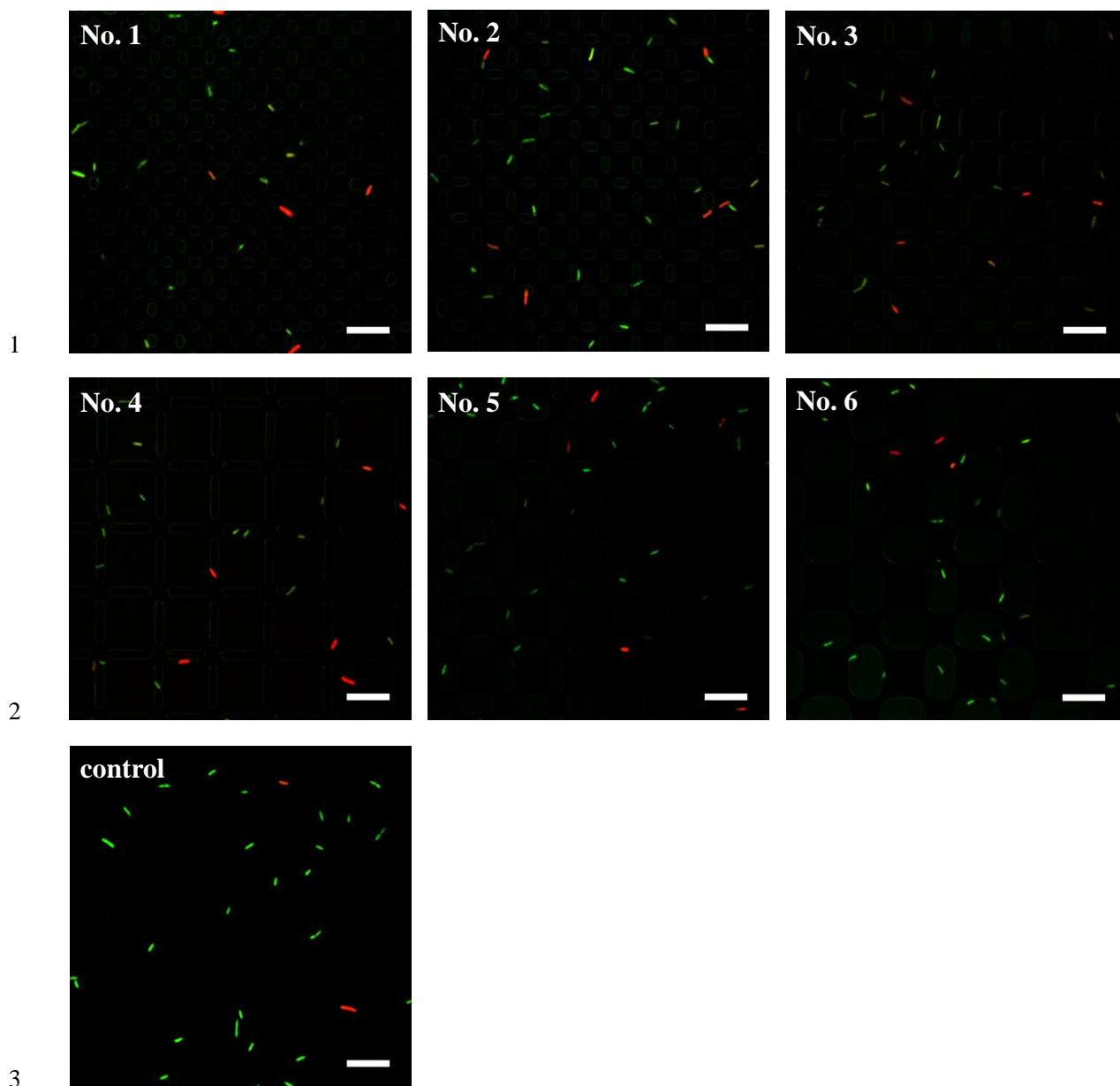
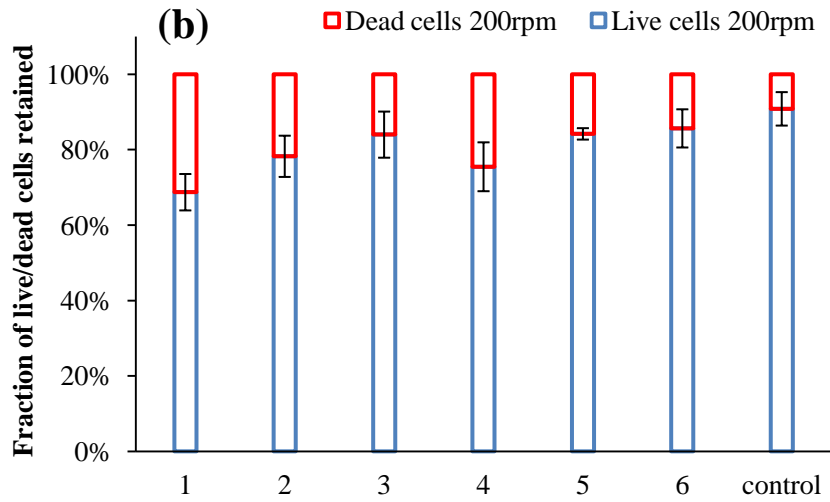
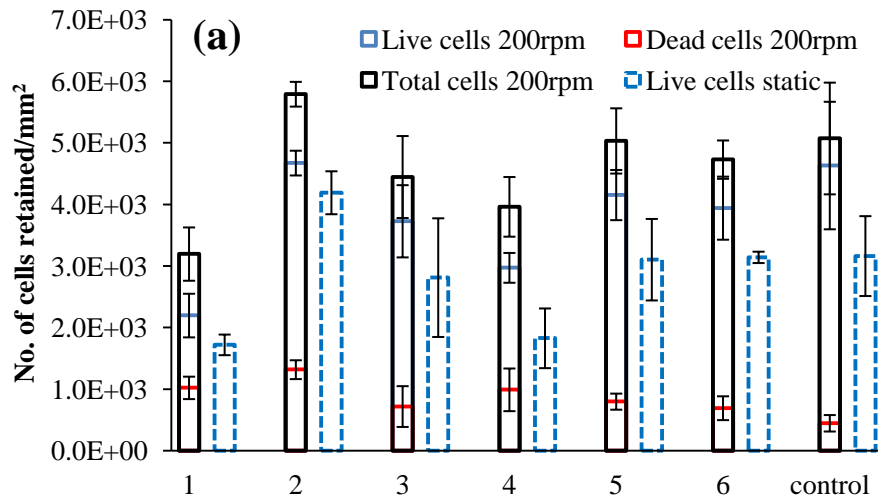


Figure 4. (a) Infrared spectra of PET before (bare PET) and after (treated PET) hot embossing. (b) Water contact angles on micro-patterned and flat (control) PET surfaces, before and after 24 h exposure to a broth of chemicals from a filtered mature bacterial suspension. On the right, an illustration of water contact angle on flat PET surface, i.e.  $\theta$  in the image.



1  
 2  
 3  
 4  
 5 **Figure 5.** CLSM fluorescence images of *E.coli* MG1655 cells attached on the patterned and flat (control)  
 6 PET surfaces after 0.5 h exposure to bacterial suspension in LB culture media at 37 °C, with shaking at 200  
 7 rpm. Scale bar, 10 μm. Live and dead cells are stained with green and red, respectively.  
 8



1

2

3

4

5

6

7

8

**Figure 6.** (a) Average numbers of live (blue), dead (red) and total (black) *E.coli* MG1655 cells attached on the patterned and flat (control) PET surfaces after 0.5 h exposure to bacterial suspension in LB culture media at 37 °C in both static and dynamic (shaking at 200 rpm) conditions. (b) The fraction of live (blue) and dead (red) cells accounting for total adherent cells in each patterned and flat surface in LB culture media. There are no dead cells attached in the static condition. The data are obtained by analyzing CLSM fluorescence images using Image J. Error bars show standard deviations.

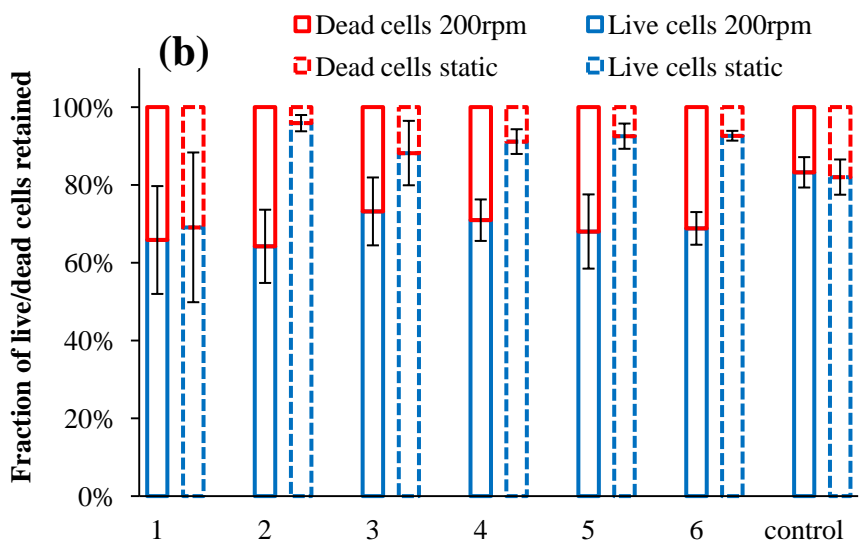
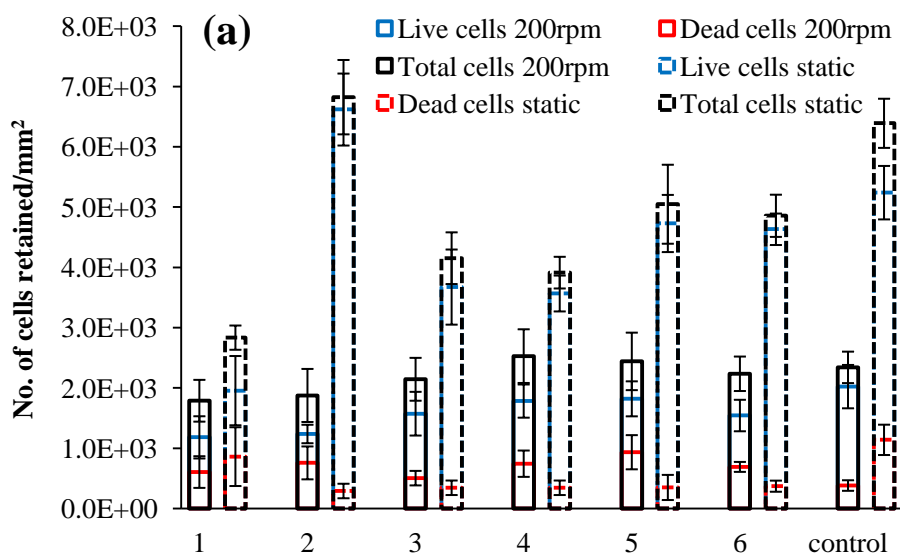
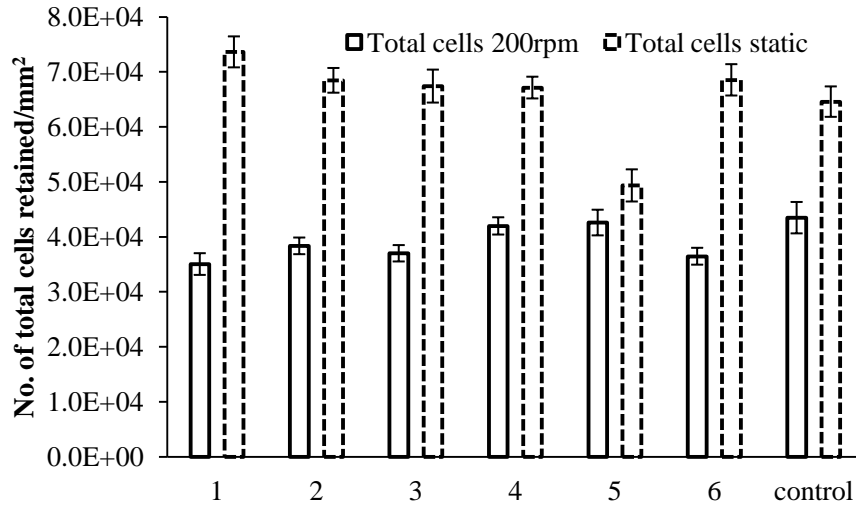
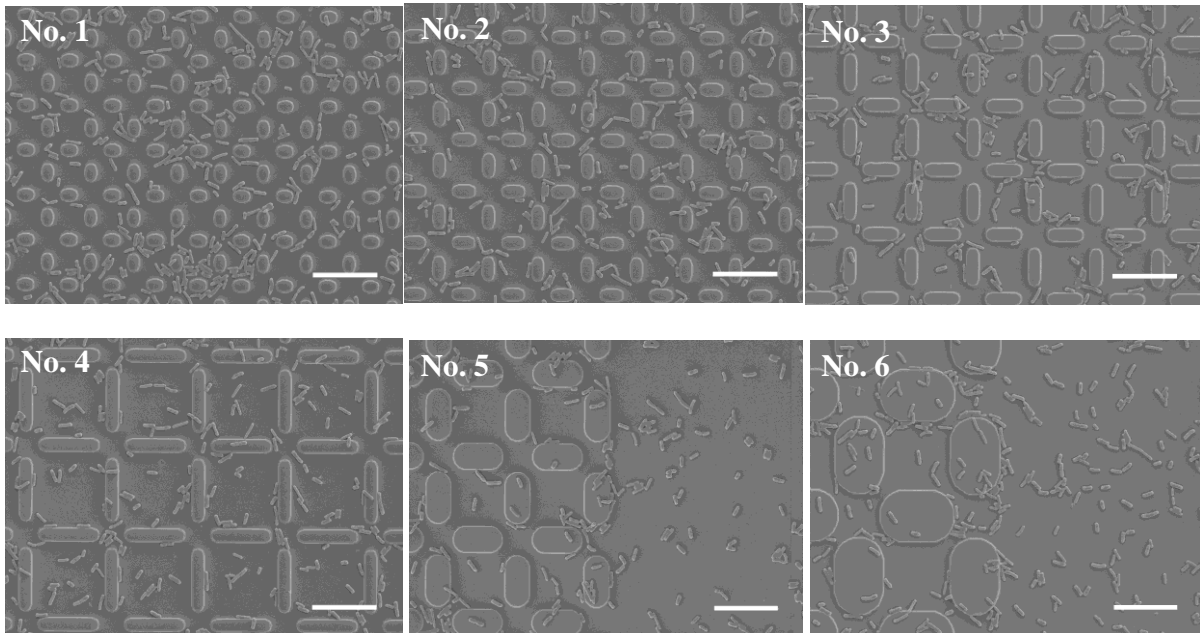


**Figure 7.** (a) Average numbers of live (blue), dead (red) and total (black) *E.coli* MG1655 cells attached on the patterned and flat (control) PET surfaces after 0.5 h exposure to bacterial suspension in PBS buffer at 37 °C in both static and dynamic (shaking at 200 rpm) conditions. (b) The fraction of live (blue) and dead (red) cells accounting for total adherent cells in each patterned and flat surface in PBS buffer. The data are obtained by analyzing CLSM fluorescence images using Image J. Error bars show standard deviations.



1  
2  
3  
4  
5  
6  
7  
8  
9

**Figure 8.** Average numbers of total *E.coli* MG1655 cells attached on the patterned and flat (control) PET surfaces after 24 h incubation in PBS-buffered bacterial suspension at 37 °C in both static and dynamic (shaking at 200 rpm) conditions. The data are obtained by analyzing CLSM fluorescence images using Image J. Error bars show standard deviations.



10  
11  
12  
13  
14  
15

**Figure 9.** Representative SEM images of *E.coli* MG1655 adhesion on patterned and flat (control) PET surfaces, after 24 h static incubation in PBS-buffered bacterial suspension at 37 °C. No. 5 and 6 images, in addition, show the boundary between the patterned area and flat region. Scale bar, 10 μm.



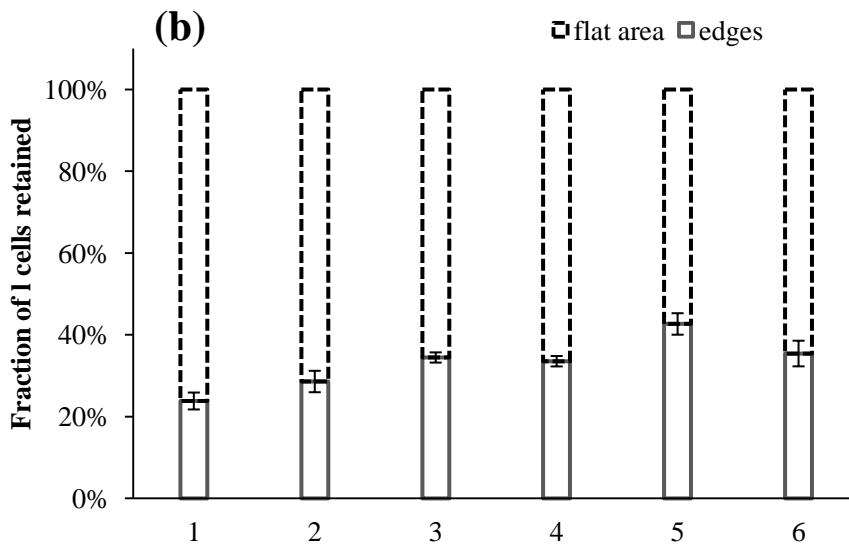
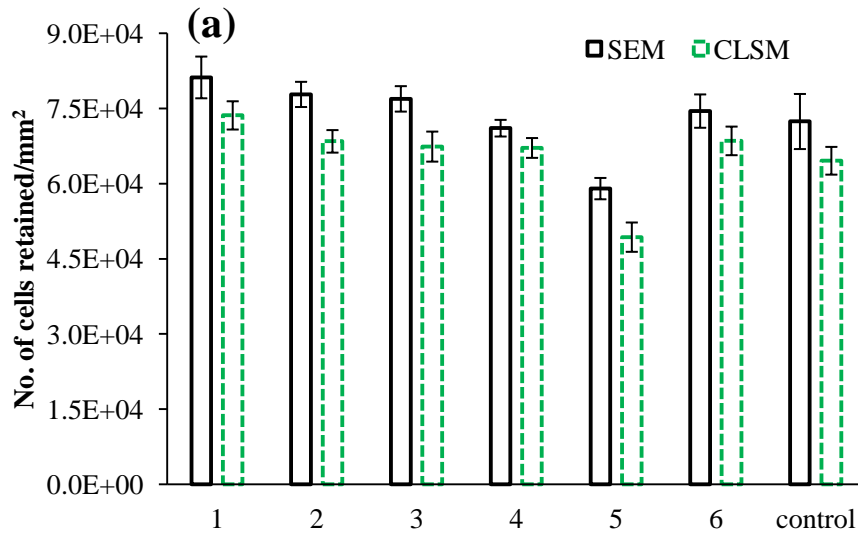
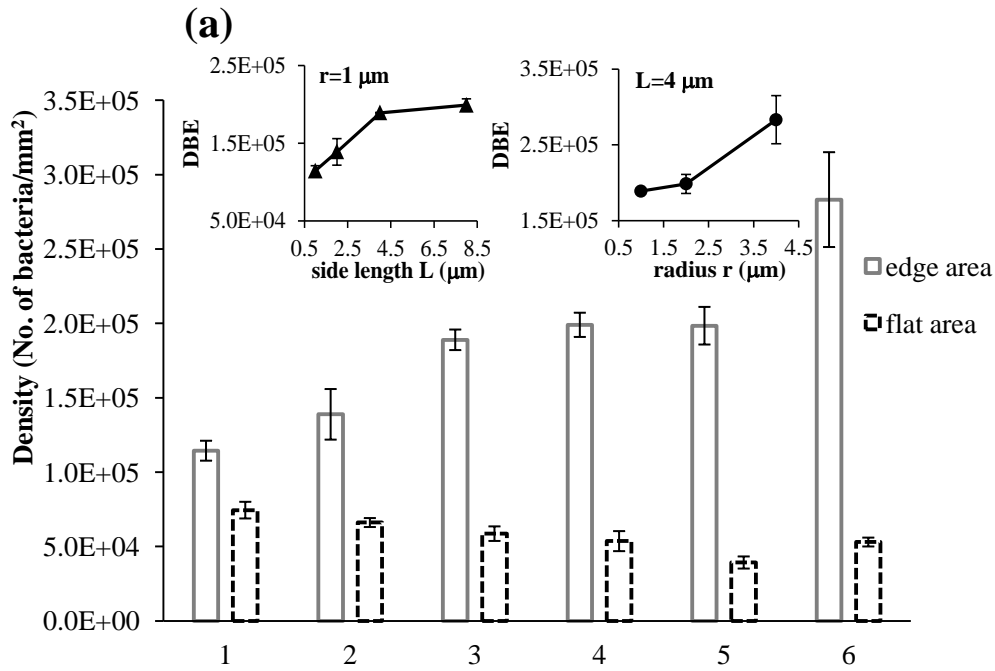
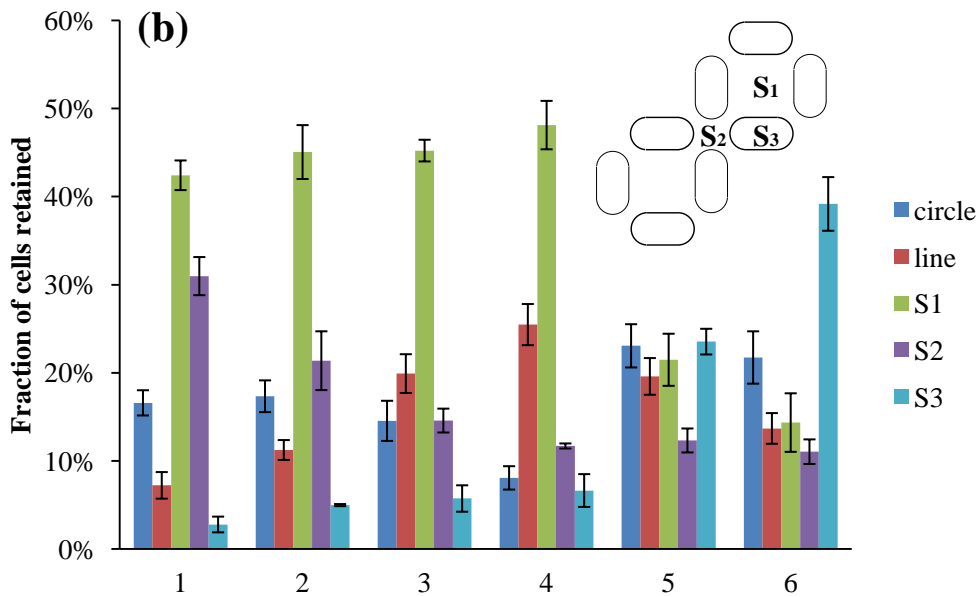


**Figure 10.** Extensive (overall) characterization of bacterial attachment to the patterned PET surfaces by analyzing SEM images. (a) Average numbers of total *E.coli* MG1655 cells adherent on the patterned and flat (control) PET surfaces after 24 h static incubation in PBS-buffered bacterial suspension at 37 °C. The black solid lines show the statistical analysis of SEM images of attached bacteria. The green dashed lines show the CLSM data (i.e. data in Figure8 presented with dashed lines) for comparison. (b) The fraction of cells attached on the edges or flat area accounting for total adherent cells.



1



2

3 **Figure 11.** Intensive (specific) characteristics of bacterial attachment on the patterned PET surfaces by  
 4 analyzing SEM images. (a) Density of bacteria retained at the edge area (DBE) and the remaining flat area.  
 5 Insets describe how the dimensions of topographic feature influence the density of bacterial occurring on the  
 6 edge area. (b) The locational fraction of bacteria retained on different parts of patterns accounting for total  
 7 adherent cells.

8